Supporting Information

Planar Pentacoordinate Silicon and Germanium Atoms

Meng-hui Wang,[a] Xue Dong,[a] Zhong-hua Cui,[a,*] Mesías Orozco-Ic,[b] Yi-hong Ding,[c,*]

Jorge Barroso,[b,*] and Gabriel Merino.[b,*]

[a]*Institute of Atomic and Molecular Physics, Jilin University, Changchun 130023, People's Republic of China; Beijing National Laboratory for Molecular Sciences*

[b]*Departamento de Física Aplicada, Centro de Investigación y de Estudios Avanzados, Unidad Mérida*

[c]*Institute of Theoretical Chemistry, Jilin University, Changchun 130023, People's Republic of China*

KEYWORDS. Planar pentacoordinate silicon, Planar pentacoordinate germanium, Global minimum, Localization, Potential energy surfaces.

E-mail: yhdd@jlu.edu.cn
E-mail: jorge.barroso@cinvestav.mx
E-mail: gmerino@cinvestav.mx
E-mail: zcui@jlu.edu.cn

Computational details

An exhaustive exploration of the potential energy surface (PES) of XMg_5^{2-}, XMg_4Y^- (X=Si, Ge; Y=Al, Ga, In, Tl), and $SiMg_3In_2$ in their singlet and triplet spin states was performed using the grid-based isomeric strategy,[1,2] and the PSO algorithm as implemented in the CALYPSO code.[3,4] An initial screening at the B3LYP/def2-SVP[5] level was made and the resulting low-lying (<20 kcal/mol above the putative global minimum) isomers were further optimized using the def2-TZVP basis set.[5] Single-point calculations for the low-lying energy isomers were performed at the CCSD(T)[6]/def2-TZVP//B3LYP/def2-TZVP[5] level. A further optimization of the lower-lying energy structures was carried out at the TPSS-D3/def2-TZVP[7,8] level and energy corrected with a single-point at CCSD(T)/def2-TZVP.[5,6] So, the structural, bonding, and energy values for the cluster discussed in the main text are those obtained at the CCSD(T)/def2-TZVP[5,6]//TPSS-D3/def2-TZVP.[7,8] To gain a better insight into the chemical bonding, the natural bonding orbital (NBO)[9–11] analysis was performed. The partial third-order (P3) self-energy approximation of the electron propagator was employed to compute the vertical electron detachment energies (VDEs). All valence orbitals were retained in the P3/def2-TZVP//TPSS-D3/def2-TZVP determinations of VDEs, with a pole strength value above the 0.8 threshold value for reliability.[12,13] All these calculations were done with the Gaussian09 program.[14]

In addition, the induced magnetic field[15-17] ($\mathbf{B}^{ind}$) and the induced current-density[18-20] analysis was carried out using the Aromagnetic[21] and GIMIC[18-20] programs, respectively. The molecular magnetic response to a homogeneous external magnetic field is calculated in a rectangular grid where the molecule is located. These magnetic calculations were performed at the PW91/def2-TZVP[22] level.

Finally, to verify the kinetic stability of the ppX clusters, Born-Oppenheimer molecular dynamics (BOMD) simulations were carried out at the PBE/DZVP[23,24] level for 10 ps, and with and a step size of 0.5 fs from the equilibrium global minimum structure. The velocities were randomly assigned to the atoms according to a Maxwell-Boltzmann distribution at 300K. These simulations were performed using the CP2K software package.[25]

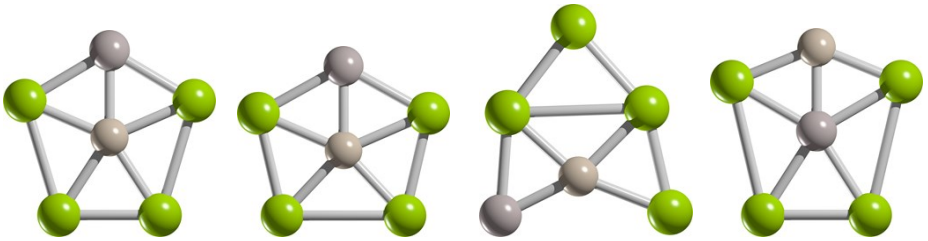

	ppX C_{2v}, $^1A_1$	ppX C_{2v}, $^3B_1$	ptX C_s, $^1A'$	ppY C_s, $^1A'$
$SiMg_4Al^-$	0.0 (0.0)	4.2 (4.2)	3.6 (3.5)	-0.2 (-0.4)
$GeMg_4Al^-$	0.0 (0.0)	4.0 (3.9)	2.1 (1.8)	-1.7 (-2.1)
$SiMg_4Ga^-$	0.0 (0.0)	4.0 (3.9)	4.5 (4.3)	0.0 (-0.2)
$GeMg_4Ga^-$	0.0 (0.0)	3.5 (3.6)	3.1 (2.9)	-1.6 (-1.9)
$SiMg_4In^-$	0.0 (0.0)	3.1 (3.0)	3.7 (3.5)	4.4 (4.4)
$GeMg_4In^-$	0.0 (0.0)	2.9 (2.8)	2.4 (2.2)	2.8 (2.8)
$SiMg_4Tl^-$	0.0 (0.0)	2.3 (2.3)	3.9 (3.8)	6.0 (6.0)
$GeMg_4Tl^-$	0.0 (0.0)	2.0 (1.9)	3.0 (2.8)	4.8 (4.6)

Figure S1. The low-lying isomers of the XMg_4Y^- species. The relative energy is in kcal/mol computed at the CCSD(T)/def2-TZVP//TPSS-D3/def2-TZVP level and at the CCSD(T)/def2-TZVP//B3LYP/def2-TZVP level between (in parentheses).

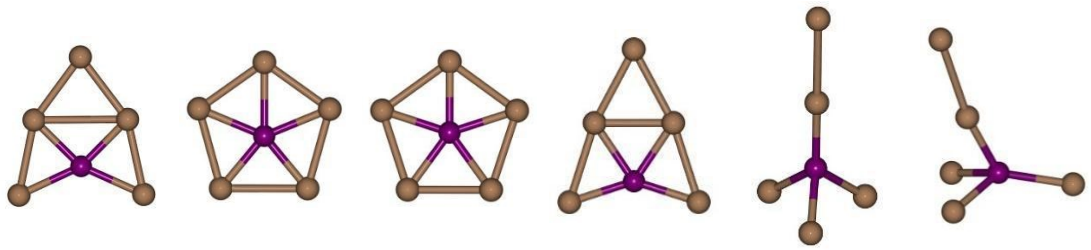

0.0	0.0	0.3	6.8	8.1	9.4
C_{2v}, $^1A_1$	C_{2v}, $^1A_1$*	D_{5h}, $^3A_1$'	C_{2v}, $^3B_2$	C_{3v}, $^3A_1$	C_s, ^{3}A"
(0.03)	(0.07)	(0.10)	(0.09)	(0.05)	(0.11)

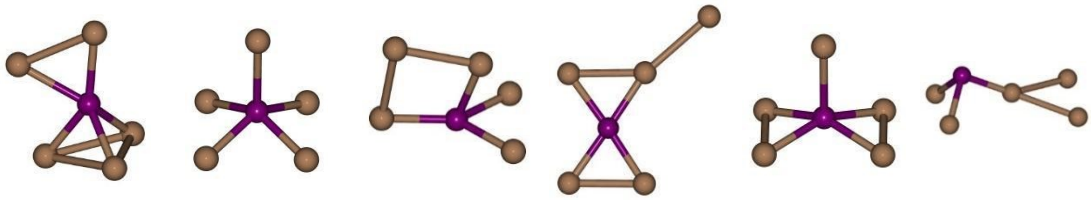

5.8	7.4	7.5	9.2	6.0	11.2
C_s, ^{3}A"	C_{4v}, $^3A_1$	C_s, ^{3}A"	C_s, ^{1}A'	C_s, ^{1}A'	C_1, ^{3}A
(0.09)	(0.05)	(0.09)	(0.03)	(0.04)	(0.10)

Figure S2. Relative energies (in kcal/mol) of the low-lying isomers of $SiMg_5^{2-}$ computed at the CCSD(T)/def2-TZVP//B3LYP/def2-TZVP level. The T1-Diagnostic values are between parentheses. "*" indicates that the structure was obtained at the UB3LYP/def2-TZVP level with broken-symmetry method.

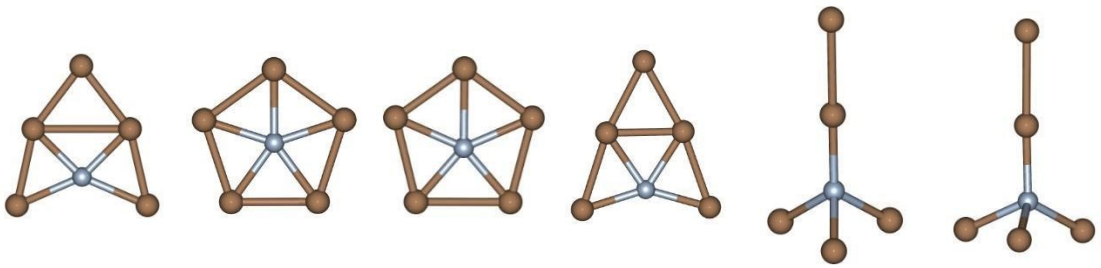

0.0 1.5 1.2 6.5 8.5 9.1

C_{2v}, $^1A_1$ D_{5h}, $^3A_1'$ C_{2v}, $^1A_1$* C_{2v}, $^3B_2$ C_{3v}, $^3A_1$ C_s, $^3A''$

(0.02) (0.08) (0.06) (0.07) (0.04) (0.08)

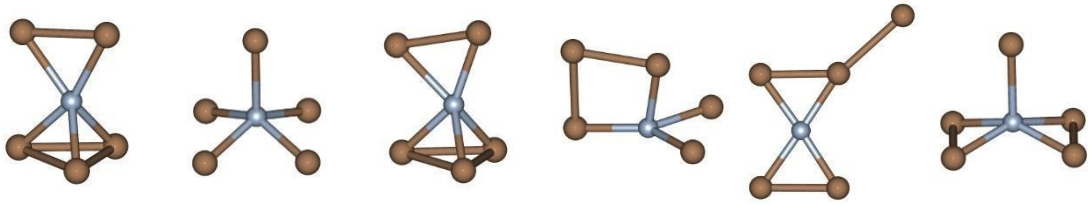

6.7 7.2 6.4 7.1 9.4 6.1

C_s, $^3A''$ C_{4v}, $^3A_1$ C_s, $^3A''$ C_s, $^3A''$ C_s, $^1A'$ C_{2v}, $^1A_1$

(0.08) (0.04) (0.07) (0.06) (0.03) (0.03)

Figure S3. Relative energies (kcal/mol) of the low-lying isomers of $GeMg_5^{2-}$ computed at the CCSD(T)/def2-TZVP//B3LYP/def2-TZVP level. The T1-Diagnostic values are between parentheses. "*" indicates that the structure was obtained at the UB3LYP/def2-TZVP level with broken-symmetry method.

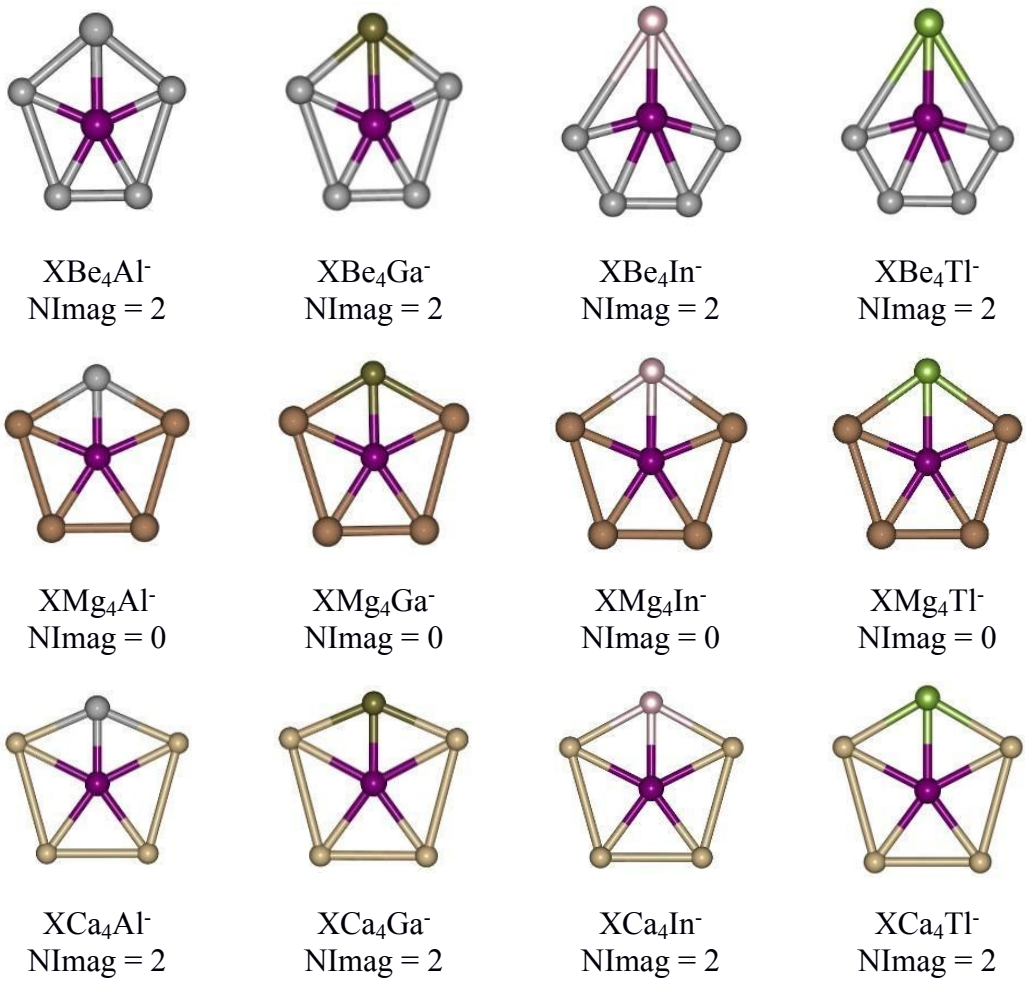

Figure S4. Structures of the XM_4Y^- species (X=Si, Ge; M=Be, Mg, Ca; Y=Al, Ga, In, Tl) optimized at the B3LYP/def2-TZVP level. NImag refers to the number of imaginary frequencies.

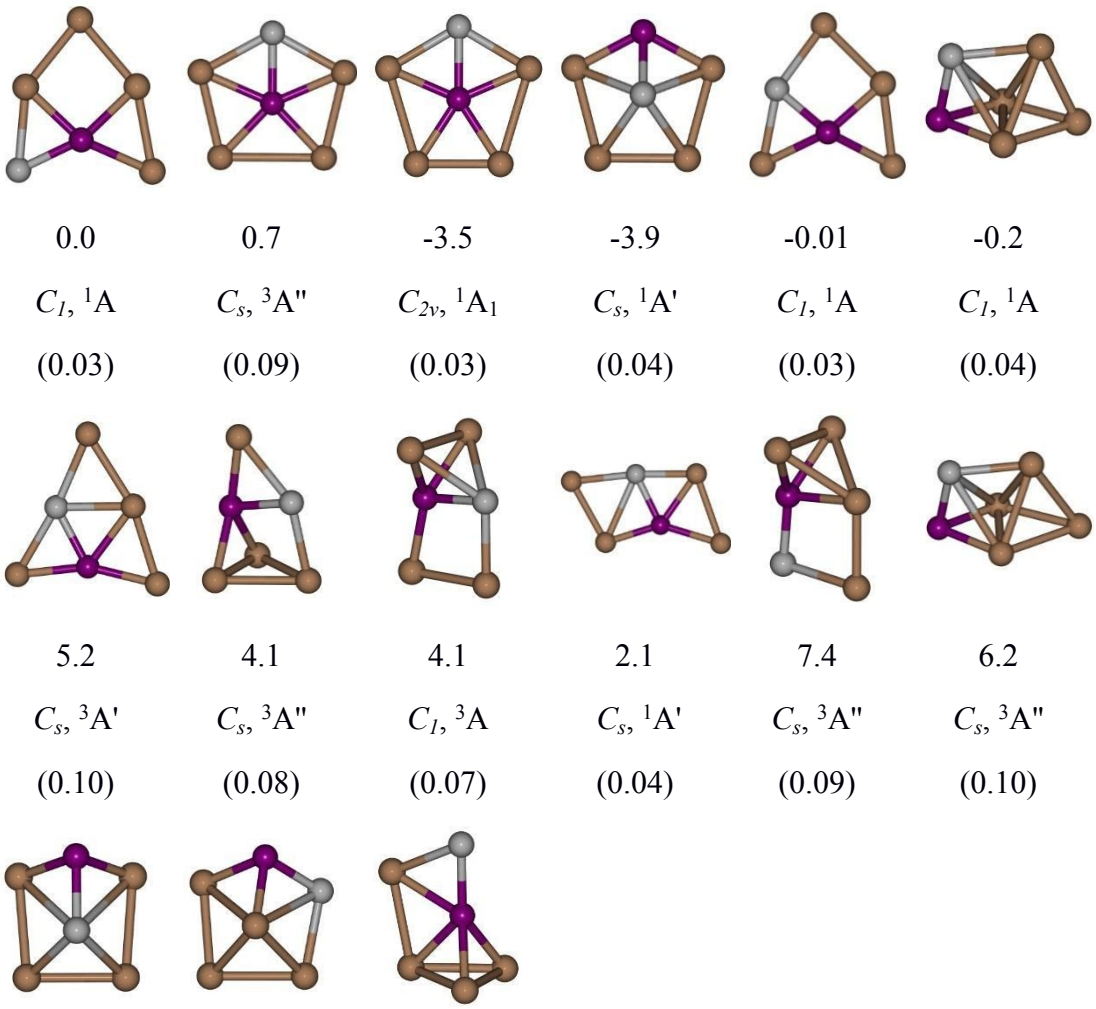

Figure S5. Relative energies (kcal/mol) of the low-lying isomers of $SiMg_4Al^-$ computed at the CCSD(T)/def2-TZVP//B3LYP/def2-TZVP level. The T1-Diagnostic values are between parentheses.

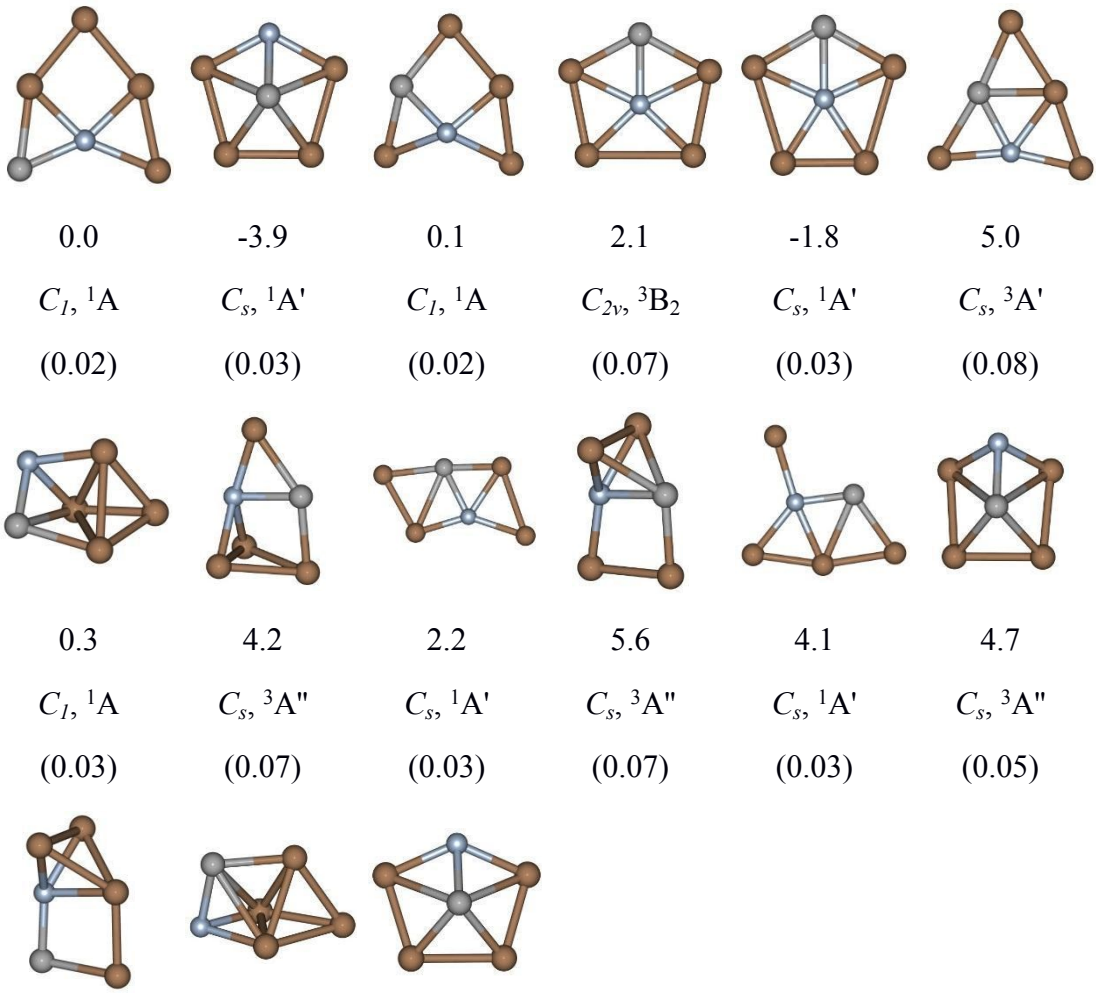

Figure S6. Relative energies (kcal/mol) of the low-lying isomers of $GeMg_4Al^-$ computed at the CCSD(T)/def2-TZVP//B3LYP/def2-TZVP level. The T1-Diagnostic values are between parentheses.

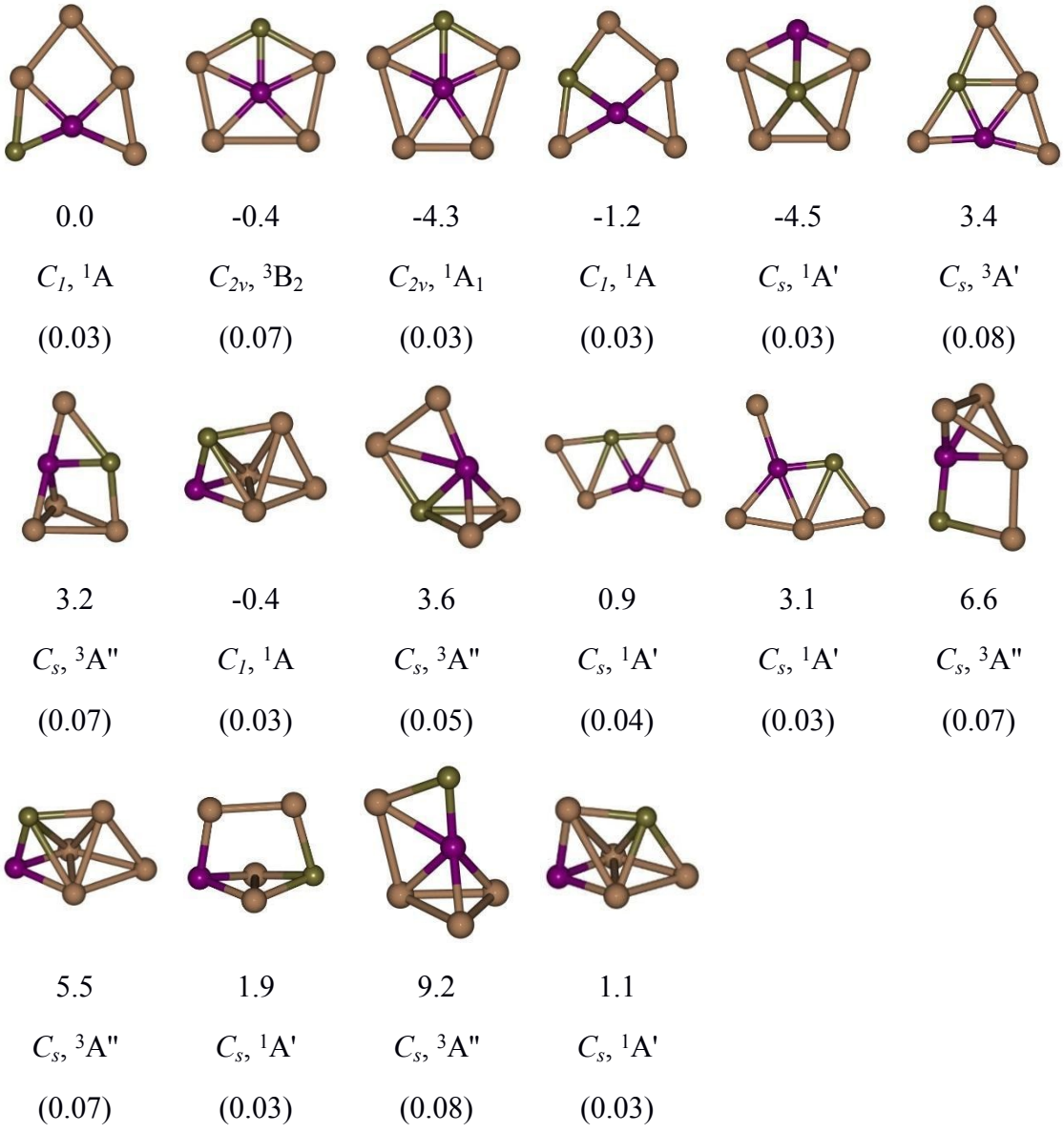

Figure S7. Relative energies (kcal/mol) of the low-lying isomers of $SiMg_4Ga^-$ computed at the CCSD(T)/def2-TZVP//B3LYP/def2-TZVP level. The T1-Diagnostic values are between parentheses.

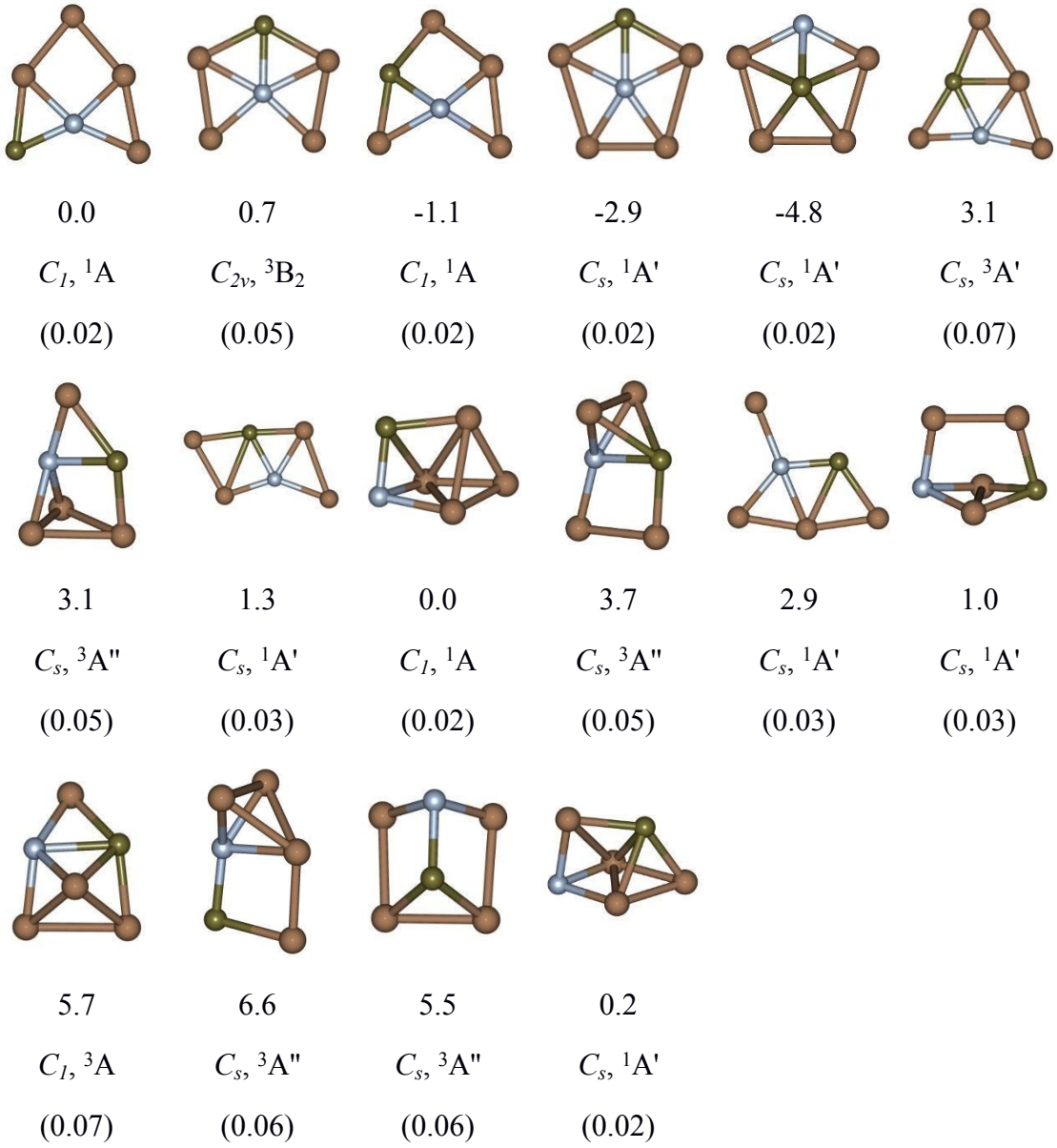

Figure S8. Relative energies (kcal/mol) of the low-lying isomers of $GeMg_4Ga^-$ computed at the CCSD(T)/def2-TZVP//B3LYP/def2-TZVP level. The T1-Diagnostic values are between parentheses.

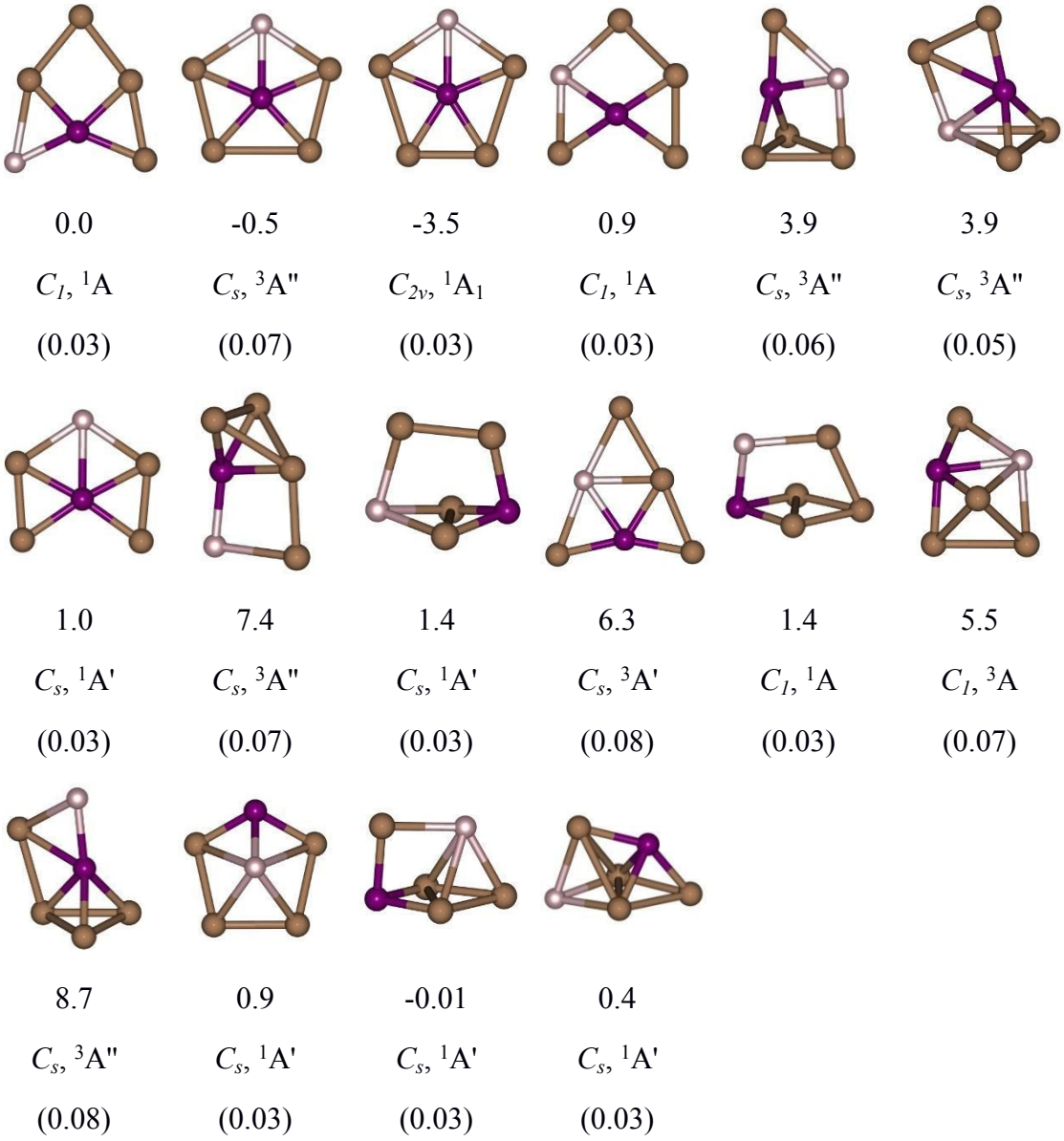

Figure S9. Relative energies (kcal/mol) of the low-lying isomers of $SiMg_4In^-$ computed at the CCSD(T)/def2-TZVP//B3LYP/def2-TZVP level. The T1-Diagnostic values are between parentheses.

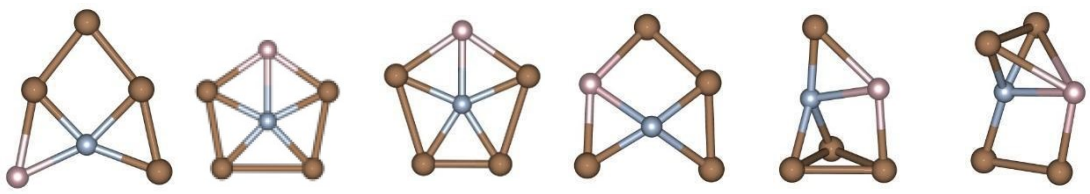

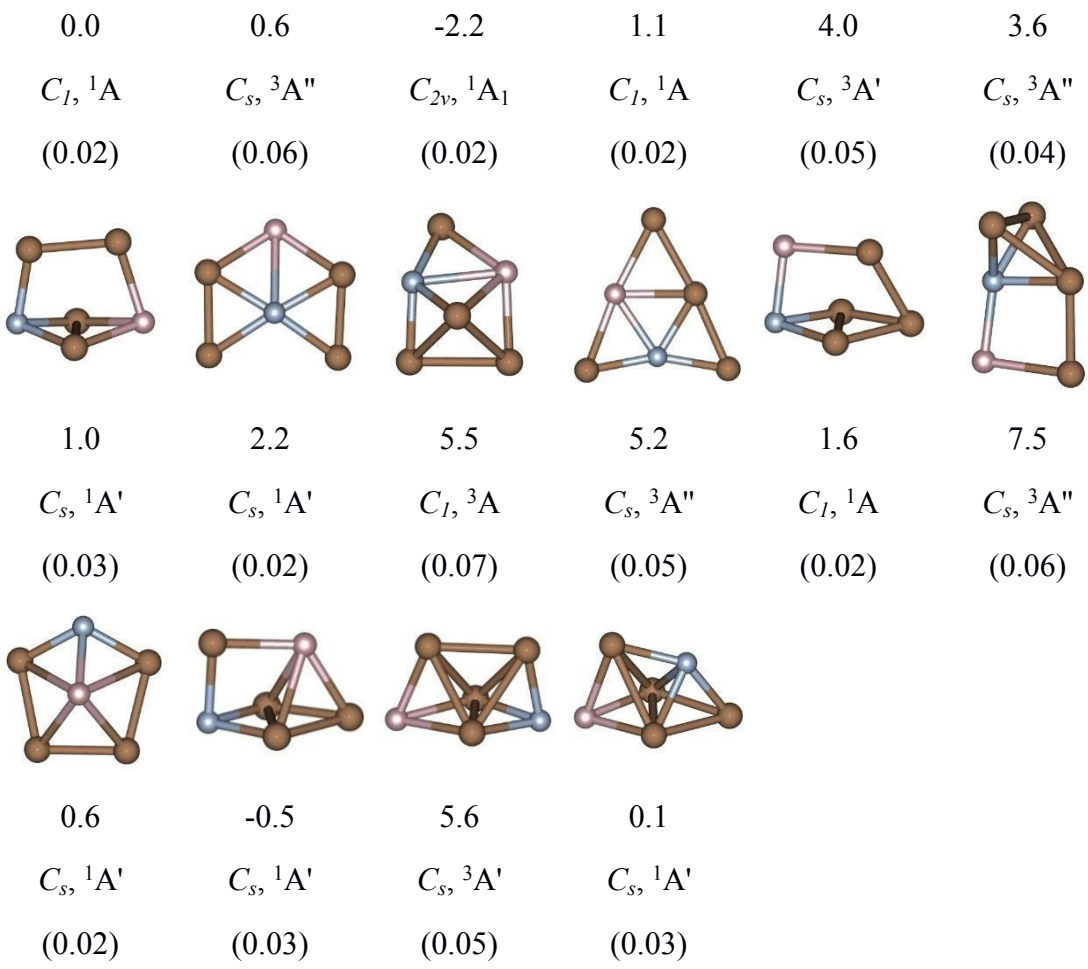

Figure S10. Relative energies (kcal/mol) of the low-lying isomers of $GeMg_4In^-$ computed at the CCSD(T)/def2-TZVP//B3LYP/def2-TZVP level. The T1-Diagnostic values are between parentheses.

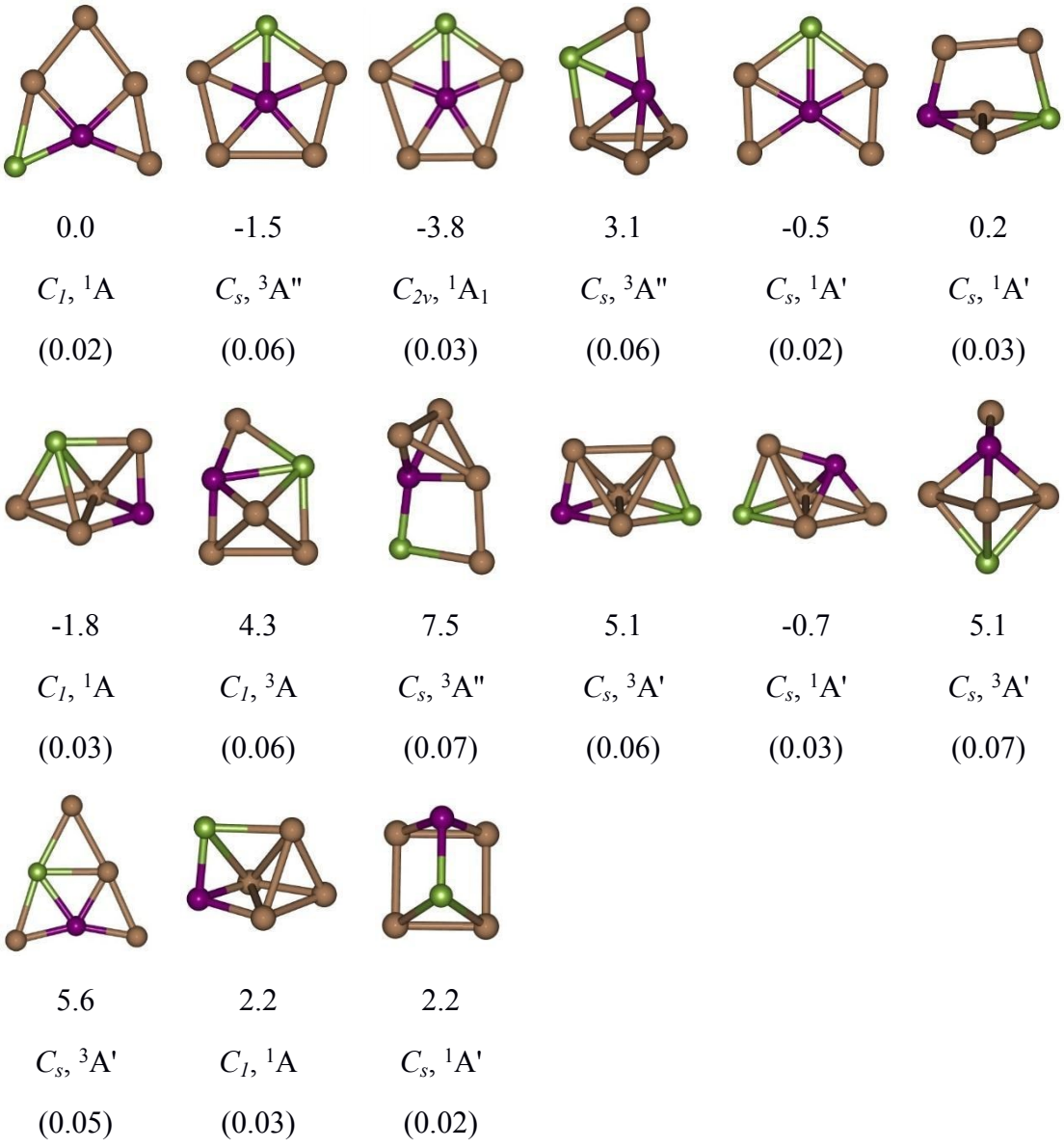

Figure S11. Relative energies (kcal/mol) of the low-lying isomers of $SiMg_4Tl^-$ computed at the CCSD(T)/def2-TZVP//B3LYP/def2-TZVP level. The T1-Diagnostic values are between parentheses.

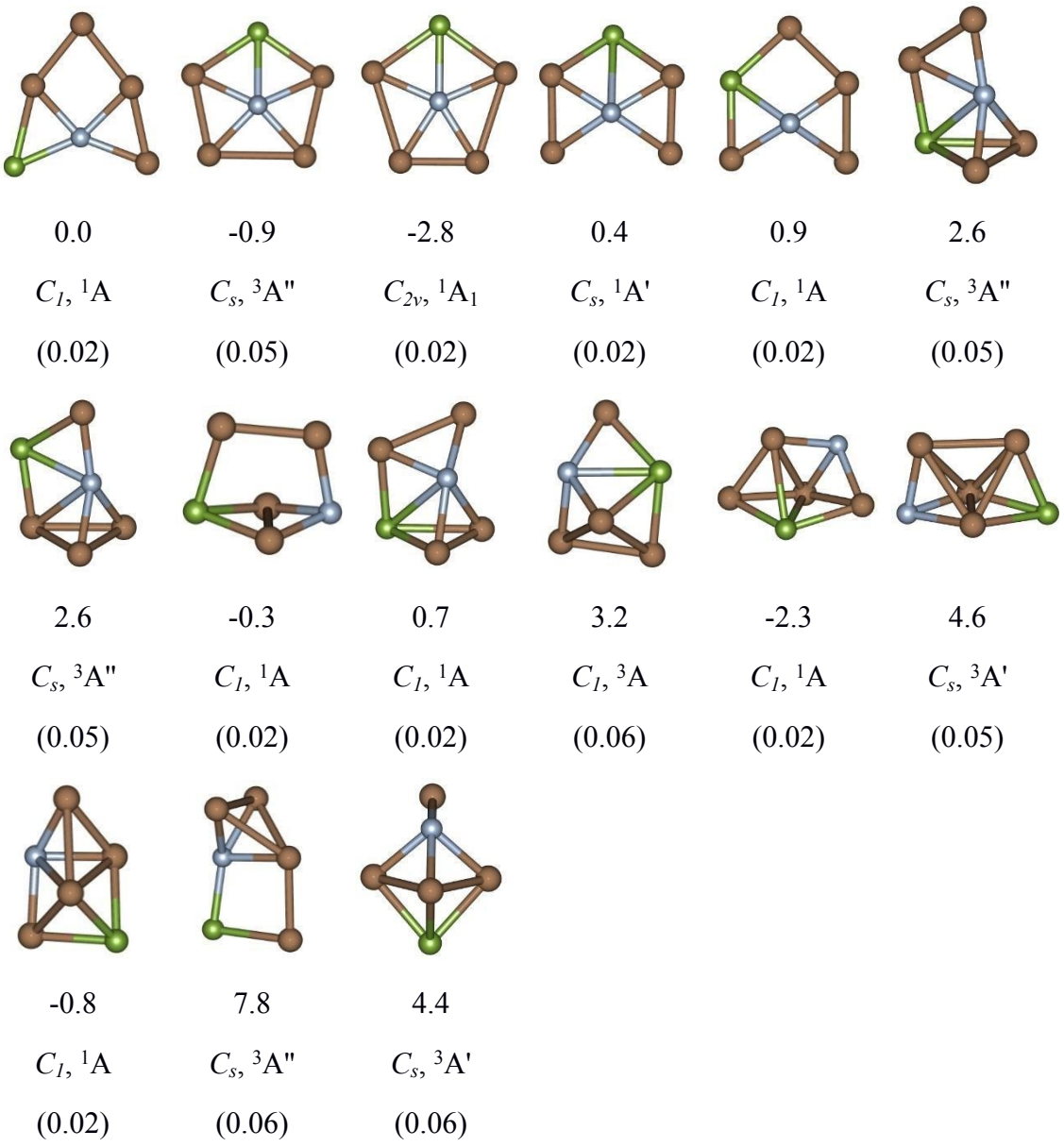

Figure S12. Relative energies (kcal/mol) of the low-lying isomers of $GeMg_4Tl^-$ computed at the CCSD(T)/def2-TZVP//B3LYP/def2-TZVP level. The T1-Diagnostic values are between parentheses.

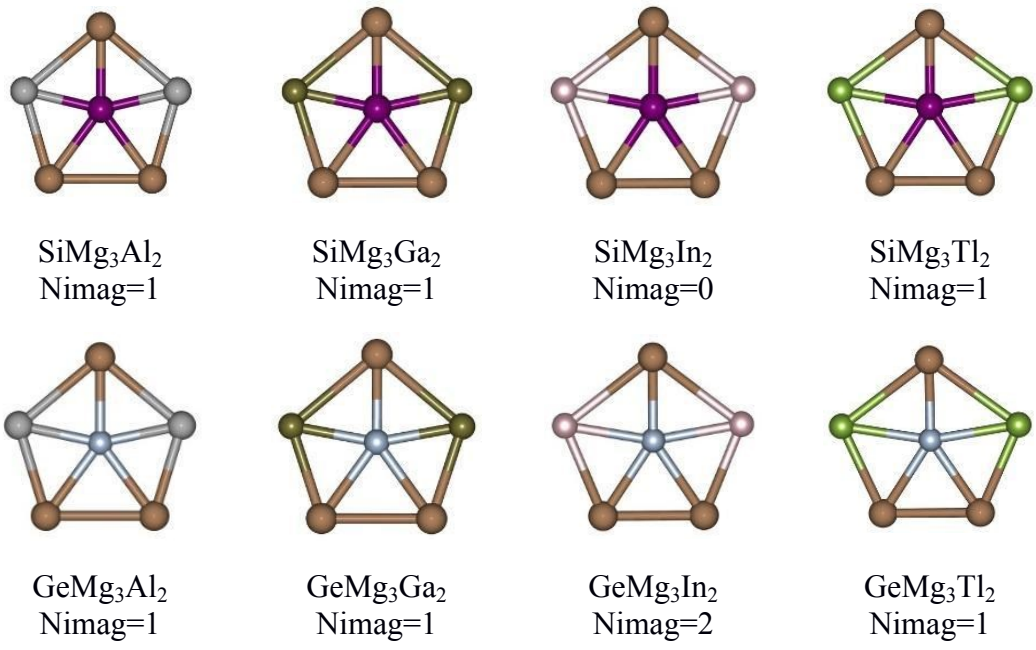

Figure S13. Structures of the XM_3Y_2 species (X=Si, Ge; M=Be, Mg, Ca; Y=Al, Ga, In, Tl) optimized at the B3LYP/def2-TZVP level. Nimag refers to the number of imaginary frequencies.

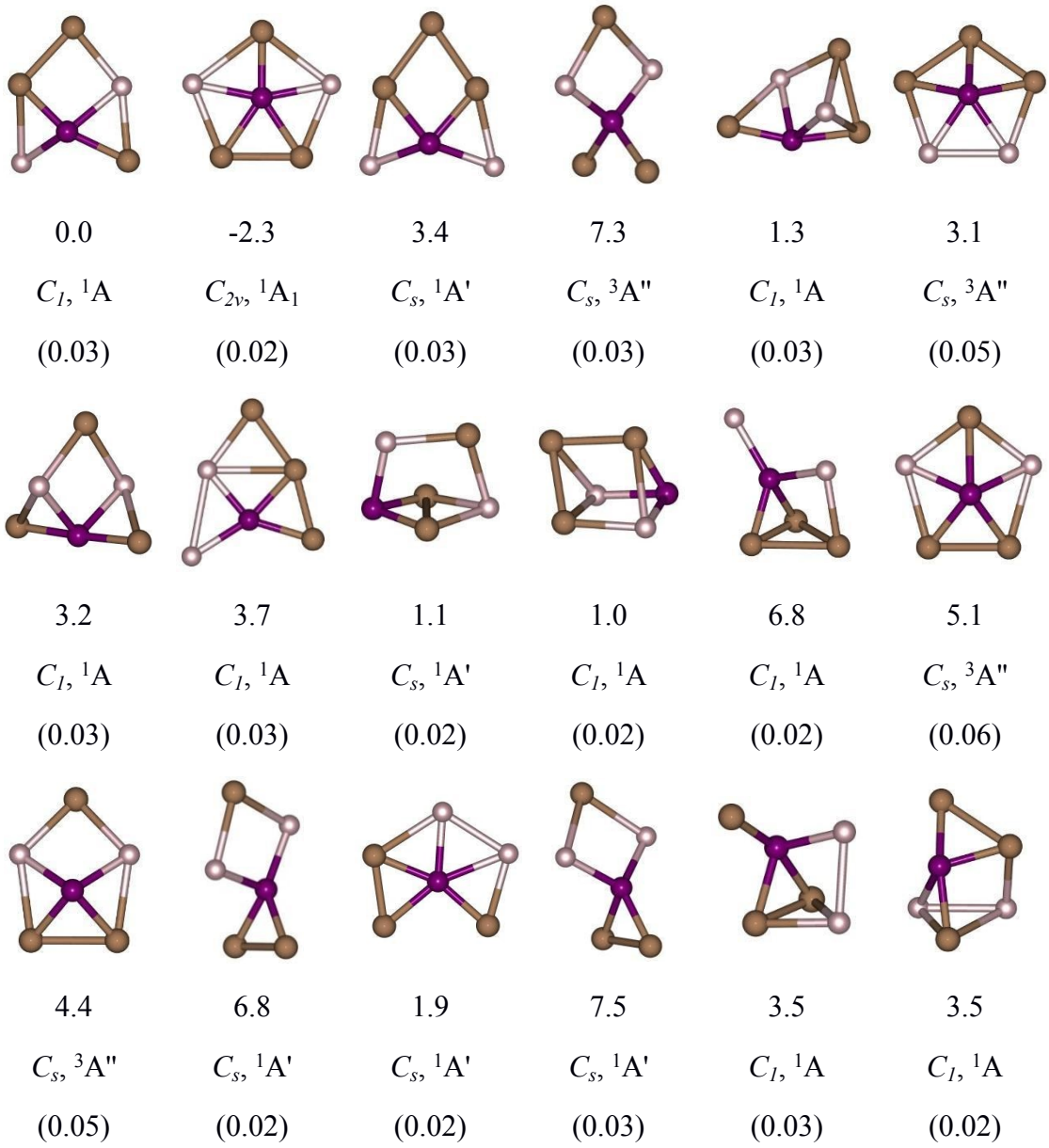

Figure S14. Relative energies (kcal/mol) of the low-lying isomers of $SiMg_3In_2$ computed at the CCSD(T)/def2-TZVP//B3LYP/def2-TZVP level. The T1-Diagnostic values are between parentheses.

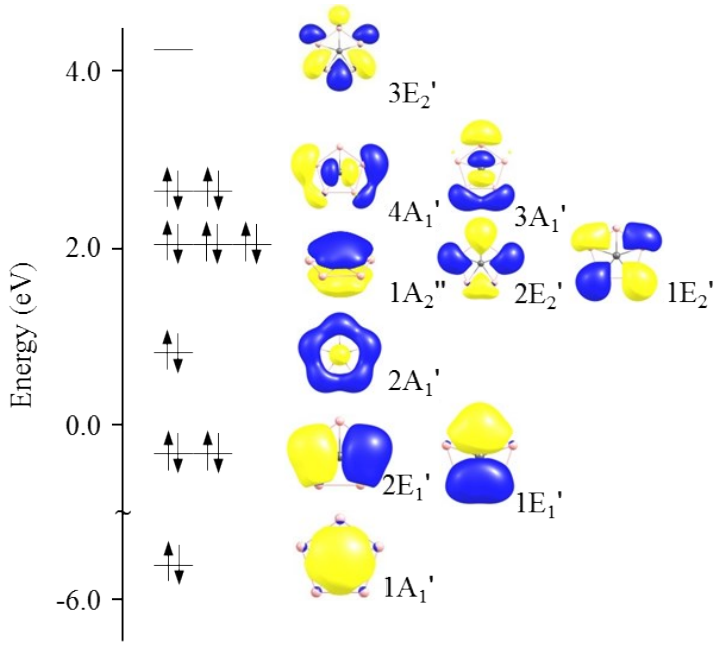

Figure S15. Molecular orbitals of the triplet $SiMg_5^{2-}$.

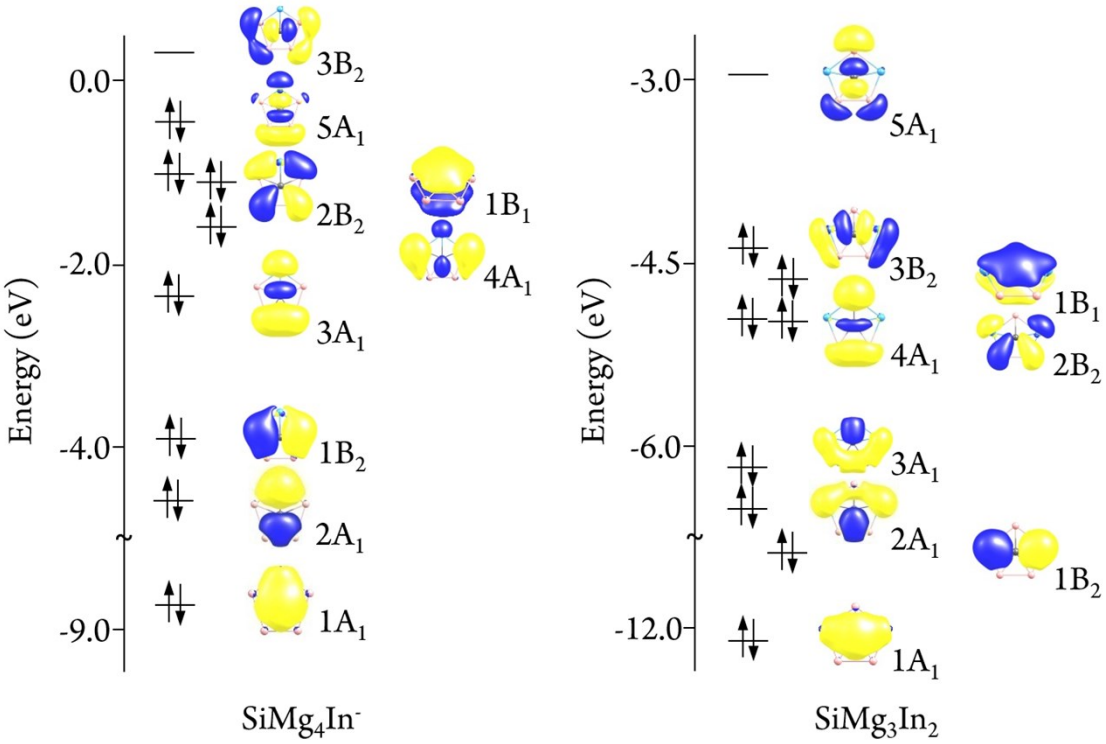

Figure S16. Molecular orbitals of the planar pentacoordinate $SiMg_4In^-$ and $SiMg_3In_2$.

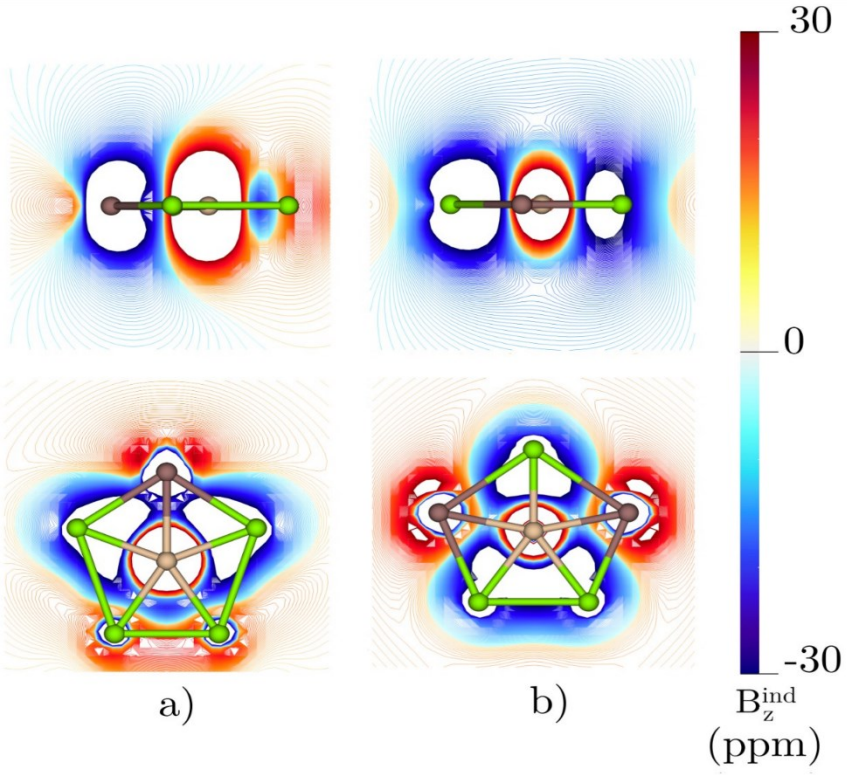

Figure S17. The B^{ind}_z isolines computed at the PW91/def2-TZVP level for a) $SiMg_4In^-$ and b) $SiMg_3In_2$

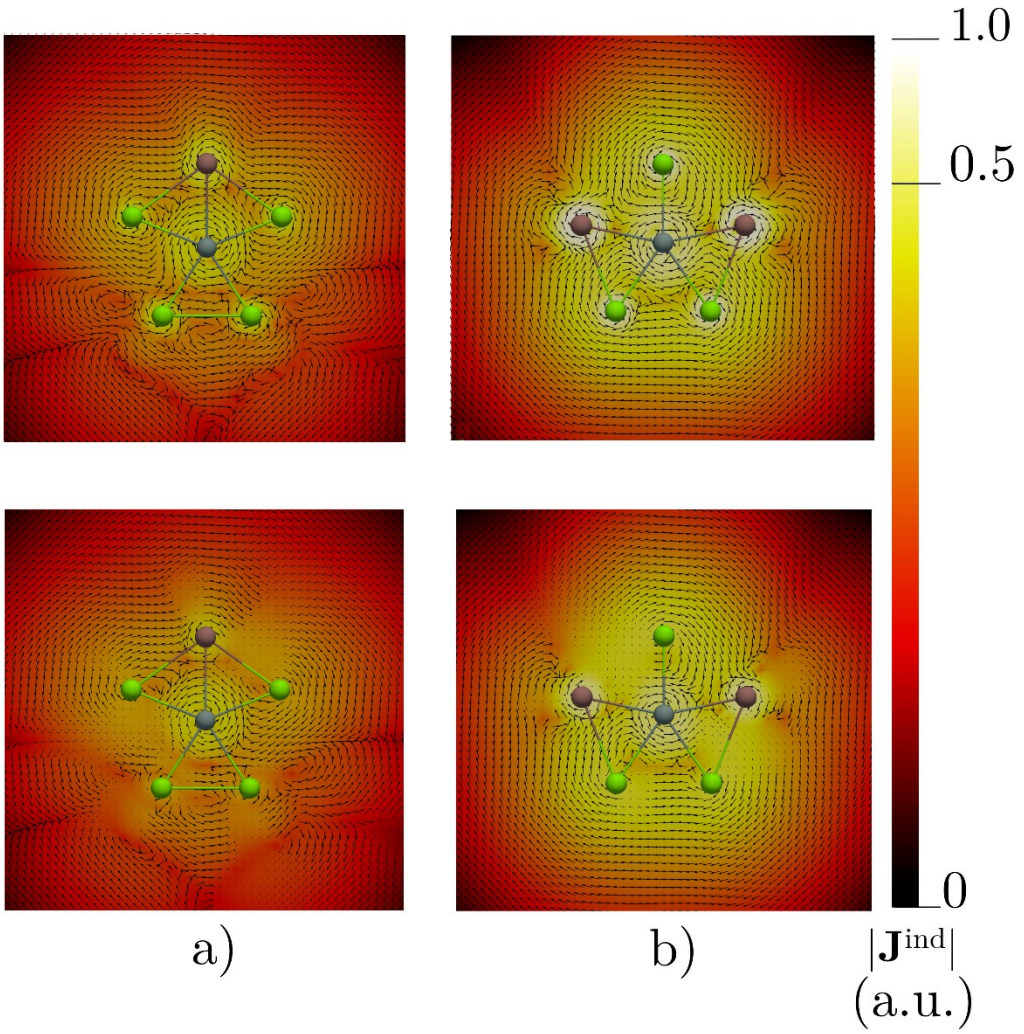

Figure S18. The induced current-density ($\mathbf{J}^{ind}$) vector maps for a) $SiMg_4In^-$ and b) $SiMg_3In_2$, calculated in the molecular plane (top) and 1 bohr (bottom) above the molecular plane. The arrows indicate the direction of $\mathbf{J}^{ind}$. The $|\mathbf{J}^{ind}|$ scale is given in atomic units (1 a.u. = 100.63 nA/T/Å^2).

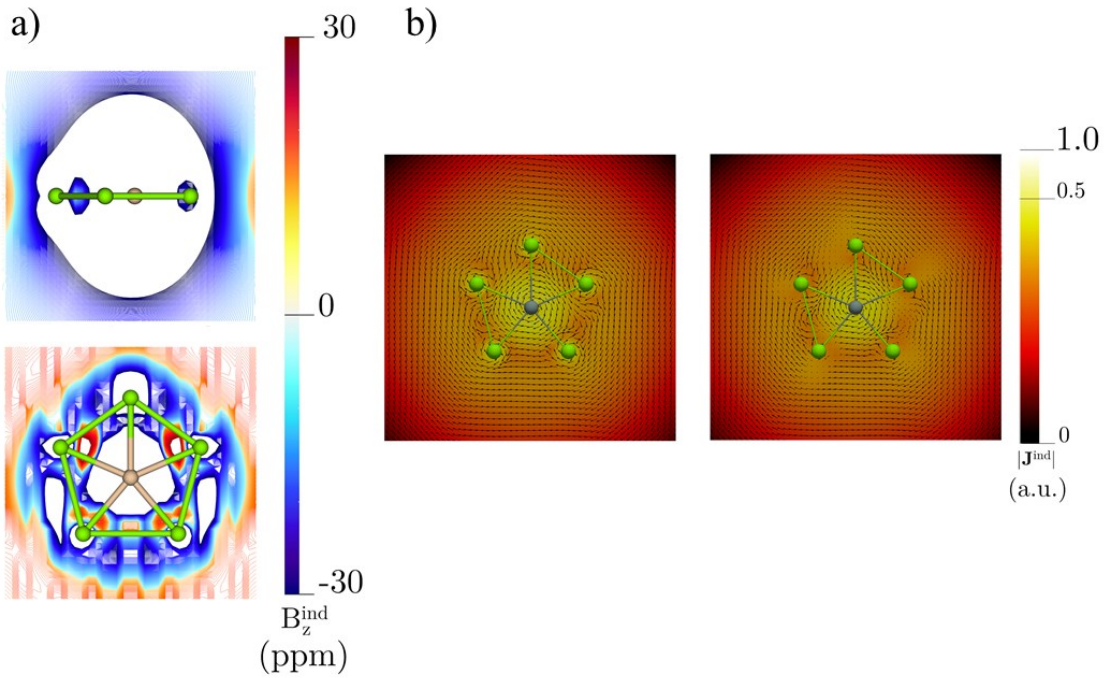

Figure S19. a) The B^{ind}_z isolines for $SiMg_5^{2-}$ and b) The induced current-density ($\mathbf{J}^{ind}$) vector maps for a) $SiMg_5^{2-}$ calculated in the molecular plane (left) and 1 bohr (right) above the molecular plane. The arrows indicate the direction of $\mathbf{J}^{ind}$. The $|\mathbf{J}^{ind}|$ scale is given in atomic units (1 a.u. = 100.63 nA/T/Å^2).

Table S1. NPA charges (Q) in |e|, bond distance (BD) in Å, and WBI values of the planar pentacoordinate isomers of XMg_5^{2-}, XMg_4Y^-, (X = Si, Ge; Y = Al, Ga, In, Tl), and $SiMg_3In_2$ at the TPSS/def2-TZVP level.

	Q_X	Q_Y	Q_{Mg}	BD_{X-Y}	BD_{X-Mg}	WBI_{X-Y}	WBI_{X-Mg}
$SiMg_5^{2-}$	-3.04	-	0.24	-	2.69	-	0.33
$GeMg_5^{2-}$	-2.84	-	0.24	-	2.76	-	0.30
$SiMg_4Al^-$	-2.46	-0.60	0.41 (0.62)	2.50	2.66 (2.63)	1.24	0.30 (0.26)
$GeMg_4Al^-$	-2.33	-0.57	0.37 (0.58)	2.55	2.67 (2.68)	1.23	0.32 (0.26)
$SiMg_4Ga^-$	-2.41	-0.70	0.43 (0.61)	2.51	2.64 (2.64)	1.28	0.32 (0.27)
$GeMg_4Ga^-$	-2.29	-0.62	0.39 (0.56)	2.57	2.67 (2.68)	1.25	0.35 (0.25)
$SiMg_4In^-$	-2.57	-0.44	0.43 (0.58)	2.74	2.63 (2.68)	1.05	0.32 (0.28)
$GeMg_4In^-$	-2.41	-0.43	0.38 (0.54)	2.79	2.67 (2.68)	1.06	0.35 (0.28)
$SiMg_4Tl^-$	-2.59	-0.39	0.43 (0.56)	2.82	2.63 (2.65)	0.99	0.33 (0.27)
$GeMg_4Tl^-$	-2.44	-0.37	0.39 (0.51)	2.88	2.66 (2.68)	1.00	0.36 (0.28)
$SiMg_3In_2$	-2.19	-0.03	0.67 (0.91)	2.70	2.69 (2.53)	0.89	0.25 (0.42)

Values between parentheses refers to the Mg connected to the Y atom.

Table S2. Smallest frequencies (ν_{min}, cm^{-1}), energy level in eV of HOMO, LUMO and HOMO–LUMO gap (Δ_{H-L}, eV) and the valence populations of Si and Ge atoms (*z*-axis is perpendicular to molecular plane, and *x*-axis is along with the direction of the substituted atoms) computed at the TPSS/def2-TZVP level.

Species	ν_{min}	HOMO	LUMO	Δ_{H-L}	Si/Ge
$SiMg_5^{2-}$	48.0	2.55	4.69	2.14	$3s^{1.97}3p_x^{1.51}3p_y^{1.51}3p_z^{1.87}$
$SiMg_4Al^-$	20.7	-0.63	0.49	1.12	$3s^{1.81}3p_x^{1.68}3p_y^{1.20}3p_z^{1.62}$
$SiMg_4Ga^-$	10.6	-0.61	0.53	1.14	$3s^{1.82}3p_x^{1.62}3p_y^{1.20}3p_z^{1.62}$
$SiMg_4In^-$	23.2	-0.62	0.49	1.11	$3s^{1.87}3p_x^{1.68}3p_y^{1.21}3p_z^{1.66}$
$SiMg_4Tl^-$	22.8	-0.58	0.52	1.10	$3s^{1.89}3p_x^{1.67}3p_y^{1.21}3p_z^{1.67}$
$GeMg_5^{2-}$	31.6	2.56	4.66	2.10	$4s^{1.97}4p_x^{1.44}4p_y^{1.44}4p_z^{1.78}$
$GeMg_4Al^-$	9.5	-0.64	0.51	1.15	$4s^{1.84}4p_x^{1.70}4p_y^{1.09}4p_z^{1.55}$
$GeMg_4Ga^-$	-9.2	-0.62	0.56	1.18	$4s^{1.85}4p_x^{1.64}4p_y^{1.09}4p_z^{1.54}$
$GeMg_4In^-$	10.0	-0.62	0.51	1.13	$4s^{1.89}4p_x^{1.69}4p_y^{1.09}4p_z^{1.57}$
$GeMg_4Tl^-$	10.2	-0.58	0.53	1.11	$4s^{1.90}4p_x^{1.68}4p_y^{1.09}4p_z^{1.58}$
$SiMg_3In_2$	10.1	-4.42	-2.95	1.47	$3s^{1.79}3p_x^{1.53}3p_y^{1.15}3p_z^{1.60}$

Table S3. Computed electron detachment (in eV) of XMg_4Y^- (X=Si, Ge; Y=In, Tl) clusters computed at the P3/def2-TZVP level. Pole strength is given in parentheses.

Detachment from MO		$SiMg_4In^-$	$SiMg_4Tl^-$	$GeMg_4In^-$	$GeMg_4Tl^-$
HOMO	a_1	2.04 (0.84)	1.99 (0.84)	2.04 (0.84)	1.98 (0.85)
HOMO-1	a_1	2.60 (0.83)	2.56 (0.83)	2.60 (0.83)	2.56 (0.83)
HOMO-2	b_2	2.68 (0.83)	2.73 (0.82)	2.70 (0.83)	2.75 (0.82)
HOMO-3	a_1	2.97 (0.82)	2.91 (0.83)	2.91 (0.83)	2.85 (0.83)

Coordinates of ppX (Si, Ge) obtained at the TPSS-D3/def2-TZVP level.

$SiMg_5^{2-}$
D5h

12	0.839502804	2.583723959	0.000000000
12	-2.197846874	1.596829224	0.000000000
12	2.716688140	0.000000000	0.000000000
12	0.839502804	-2.583723959	0.000000000
12	-2.197846874	-1.596829224	0.000000000
14	0.000000000	0.000000000	0.000000000

$GeMg_5^{2-}$
D5h

Mg	0.852235000	2.622911000	0.000000000
Mg	2.757892000	0.000000000	0.000000000
Mg	-2.231182000	1.621048000	0.000000000
Mg	-2.231181000	-1.621048000	0.000000000
Mg	0.852236000	-2.622911000	0.000000000
Ge	0.000000000	0.000000000	0.000000000

$SiMg_4Al^-$
ptX

12	-0.108169000	-3.143515000	0.000000000
12	-1.978125000	-0.866728000	0.000000000
12	1.930007000	-0.980742000	0.000000000
12	2.487195000	1.880696000	0.000000000
13	-2.151607000	1.939642000	0.000000000
14	0.000000000	0.864866000	0.000000000

$GeMg_4Al^-$
ptX

12	-0.093032000	-3.339420000	0.000000000
12	-1.966475000	-1.062474000	0.000000000
12	1.930485000	-1.153806000	0.000000000
12	2.535056000	1.706715000	0.000000000
13	-2.220955000	1.754673000	0.000000000
32	0.000000000	0.730534000	0.000000000

$SiMg_4Ga^-$
ptX

12	2.505599000	-2.514979000	0.000000000
12	-0.385648000	-1.929862000	0.000000000
12	2.660779000	0.458159000	0.000000000
12	1.269853000	3.019806000	0.000000000
31	-2.342161000	0.075215000	0.000000000
14	0.000000000	0.662203000	0.000000000

$GeMg_4Ga^-$
ptX

12	2.485007000	-2.679182000	0.000000000

12	-0.396661000	-2.032312000	0.000000000
12	2.680230000	0.297126000	0.000000000
12	1.387020000	2.918174000	0.000000000
31	-2.382811000	-0.031444000	0.000000000
32	0.000000000	0.591534000	0.000000000

$SiMg_4In^-$
ptX

12	3.969921000	-0.564696000	0.000000000
12	1.172142000	-1.513004000	0.000000000
12	2.422885000	1.968697000	0.000000000
12	-0.063721000	3.471051000	0.000000000
49	-1.837035000	-1.056816000	0.000000000
14	0.000000000	0.817102000	0.000000000

$GeMg_4In^-$
ptX

12	3.966560000	-0.755315000	0.000000000
12	1.147845000	-1.647125000	0.000000000
12	2.488932000	1.822323000	0.000000000
12	0.046385000	3.412759000	0.000000000
49	-1.873401000	-1.170557000	0.000000000
32	0.000000000	0.730174000	0.000000000

$SiMg_4Tl^-$
ptX

12	4.253352000	1.353902000	0.000000000
12	1.972606000	-0.533229000	0.000000000
12	1.858345000	3.105448000	0.000000000
12	-0.996645000	3.611345000	0.000000000
81	-1.050023000	-1.317976000	0.000000000
14	0.000000000	1.164747000	0.000000000

$GeMg_4Tl^-$
ptX

12	4.288757000	1.136083000	0.000000000
12	1.958680000	-0.694797000	0.000000000
12	1.951429000	2.967577000	0.000000000
12	-0.892843000	3.581897000	0.000000000
81	-1.082374000	-1.456774000	0.000000000
32	0.000000000	1.065924000	0.000000000

$SiMg_4Al^-$
ppX

12	0.000000000	2.418873000	-0.980105000
12	0.000000000	1.466591000	2.271379000
13	0.000000000	0.000000000	-2.443421000
12	0.000000000	-2.418873000	-0.980105000
12	0.000000000	-1.466591000	2.271379000
14	0.000000000	0.000000000	0.055279000

$GeMg_4Al^-$
ppX
12 0.000000000 2.437331000 -1.033705000
12 0.000000000 1.473628000 2.302341000
13 0.000000000 0.000000000 -2.491771000
12 0.000000000 -2.437331000 -1.033705000
12 0.000000000 -1.473628000 2.302341000
32 0.000000000 0.000000000 0.060805000

$SiMg_4Ga^-$
ppX
12 0.000000000 2.396233000 0.550918000
12 0.000000000 1.468052000 -2.753782000
31 0.000000000 0.000000000 1.956101000
12 0.000000000 -2.396233000 0.550918000
12 0.000000000 -1.468052000 -2.753782000
14 0.000000000 0.000000000 -0.555028000

$GeMg_4Ga^-$
ppX
12 0.000000000 2.413229000 -0.671946000
12 0.000000000 1.474503000 2.715099000
31 0.000000000 0.000000000 -2.085053000
12 0.000000000 -2.413229000 -0.671946000
12 0.000000000 -1.474503000 2.715099000
32 0.000000000 0.000000000 0.487530000

$SiMg_4In^-$
ppX
12 0.000000000 2.435921000 0.057174000
12 0.000000000 1.446248000 -3.166852000
49 0.000000000 0.000000000 1.792532000
12 0.000000000 -2.435921000 0.057174000
12 0.000000000 -1.446248000 -3.166852000
14 0.000000000 0.000000000 -0.942987000

$GeMg_4In^-$
ppX
12 0.000000000 2.453867000 0.211661000
12 0.000000000 1.453769000 -3.088402000
49 0.000000000 0.000000000 1.953904000
12 0.000000000 -2.453867000 0.211661000
12 0.000000000 -1.453769000 -3.088402000
32 0.000000000 0.000000000 -0.834359000

$SiMg_4Tl^-$
ppX
12 0.000000000 2.431881000 -0.389087000
12 0.000000000 1.439474000 -3.619973000

81	0.000000000	0.000000000	1.428745000
12	0.000000000	-2.431881000	-0.389087000
12	0.000000000	-1.439474000	-3.619973000
14	0.000000000	0.000000000	-1.393634000

$GeMg_4Tl^-$
ppX

12	0.000000000	2.449670000	-0.220296000
12	0.000000000	1.445966000	-3.524329000
81	0.000000000	0.000000000	1.609776000
12	0.000000000	-2.449670000	-0.220296000
12	0.000000000	-1.445966000	-3.524329000
32	0.000000000	0.000000000	-1.266276000

$SiMg_4Al^-$
ppX-triplet

12	0.000000000	2.471331000	-0.918623000
12	0.000000000	1.784297000	2.073115000
13	0.000000000	0.000000000	-2.310206000
12	0.000000000	-2.471331000	-0.918623000
12	0.000000000	-1.784297000	2.073115000
14	0.000000000	0.000000000	0.166062000

$GeMg_4Al^-$
ppX-triplet

12	0.000000000	2.478024000	-0.999682000
12	0.000000000	1.885859000	2.031044000
13	0.000000000	0.000000000	-2.355088000
12	0.000000000	-2.478024000	-0.999682000
12	0.000000000	-1.885859000	2.031044000
32	0.000000000	0.000000000	0.183233000

$SiMg_4Ga^-$
ppX-triplet

12	0.000000000	2.436628000	0.508560000
12	0.000000000	1.827644000	-2.510286000
31	0.000000000	0.000000000	1.844047000
12	0.000000000	-2.436628000	0.508560000
12	0.000000000	-1.827644000	-2.510286000
14	0.000000000	0.000000000	-0.651718000

$GeMg_4Ga^-$
ppX-triplet

12	0.000000000	2.434980000	-0.663424000
12	0.000000000	1.951434000	2.386847000
31	0.000000000	0.000000000	-1.963301000
12	0.000000000	-2.434980000	-0.663424000
12	0.000000000	-1.951434000	2.386847000
32	0.000000000	0.000000000	0.609381000

$SiMg_4In^-$
ppX-triplet

12	0.000000000	2.472317000	0.044751000
12	0.000000000	1.750785000	-2.944744000
49	0.000000000	0.000000000	1.708726000
12	0.000000000	-2.472317000	0.044751000
12	0.000000000	-1.750785000	-2.944744000
14	0.000000000	0.000000000	-1.009124000

$GeMg_4In^-$
ppX-triplet

12	0.000000000	2.470536000	0.225438000
12	0.000000000	1.842351000	-2.811499000
49	0.000000000	0.000000000	1.868231000
12	0.000000000	-2.470536000	0.225438000
12	0.000000000	-1.842351000	-2.811499000
32	0.000000000	0.000000000	-0.921184000

$SiMg_4Tl^-$
ppX-triplet

12	0.000000000	2.457984000	-0.379127000
12	0.000000000	1.747926000	-3.381757000
81	0.000000000	0.000000000	1.364027000
12	0.000000000	-2.457984000	-0.379127000
12	0.000000000	-1.747926000	-3.381757000
14	0.000000000	0.000000000	-1.444640000

$GeMg_4Tl^-$
ppX-triplet

12	0.000000000	2.451422000	-0.180357000
12	0.000000000	1.839572000	-3.234387000
81	0.000000000	0.000000000	1.542051000
12	0.000000000	-2.451422000	-0.180357000
12	0.000000000	-1.839572000	-3.234387000
32	0.000000000	0.000000000	-1.342259000

$SiMg_4Al^-$
ppY

12	0.313520000	-0.877392000	2.260176000
12	0.313520000	2.070794000	1.461896000
14	-0.003903000	-2.099095000	0.000000000
12	0.313520000	-0.877392000	-2.260176000
12	0.313520000	2.070794000	-1.461896000
13	-1.153409000	0.057360000	0.000000000

$GeMg_4Al^-$
ppY

12	0.282695000	-0.458465000	2.288378000
12	0.282695000	2.492693000	1.459356000
32	0.046700000	-1.719203000	0.000000000

12	0.282695000	-0.458465000	-2.288378000
12	0.282695000	2.492693000	-1.459356000
13	-1.158751000	0.476385000	0.000000000

$SiMg_4Ga^-$
ppY

12	0.000000000	2.379558000	-1.105573000
12	0.000000000	1.519202000	2.341500000
14	0.000000000	0.000000000	-2.304888000
12	0.000000000	-2.379558000	-1.105573000
12	0.000000000	-1.519202000	2.341500000
31	0.000000000	0.000000000	0.084070000

$GeMg_4Ga^-$
ppY

12	0.000000000	2.392336000	0.700949000
12	0.000000000	1.514795000	-2.730446000
32	0.000000000	0.000000000	1.979538000
12	0.000000000	-2.392336000	0.700949000
12	0.000000000	-1.514795000	-2.730446000
31	0.000000000	0.000000000	-0.472170000

$SiMg_4In^-$
ppY

12	0.947991000	-2.204984000	0.928285000
12	-2.032654000	-1.483352000	0.794387000
14	2.177973000	-0.006066000	0.419366000
12	0.961627000	2.200819000	0.927425000
12	-2.022721000	1.495968000	0.792638000
49	-0.096786000	-0.000336000	-0.962938000

$GeMg_4In^-$
ppY

12	0.807899000	-0.680380000	2.242467000
12	0.807899000	2.306810000	1.488694000
32	0.333698000	-1.913520000	0.000000000
12	0.807899000	-0.680380000	-2.242467000
12	0.807899000	2.306810000	-1.488694000
49	-1.009337000	0.453027000	0.000000000

$SiMg_4Tl^-$
ppY

12	-1.272233000	-2.128181000	-1.133472000
12	1.724283000	-1.550820000	-1.365085000
14	-2.304429000	0.020469000	-0.220810000
12	-1.222376000	2.124237000	-1.178019000
12	1.762669000	1.477763000	-1.396380000
81	0.251283000	0.007870000	0.789714000

$GeMg_4Tl^-$

ppY

12	1.034151000	-2.135472000	1.102011000
12	-1.921179000	-1.422101000	1.548553000
32	2.094880000	-0.020613000	0.066561000
12	1.115003000	2.200525000	0.953477000
12	-1.852314000	1.606945000	1.437694000
81	-0.586964000	-0.028878000	-0.773219000

$SiMg_3In_2$

In	0.000000000	2.670722000	-0.338232000
Mg	0.000000000	1.543438000	2.460742000
Mg	0.000000000	0.000000000	-2.365151000
In	0.000000000	-2.670722000	-0.338232000
Mg	0.000000000	-1.543438000	2.460742000
Si	0.000000000	0.000000000	0.176481000

References

(1) C. B. Shao, Y. H. Ding, Grid-Based Comprehensive Isomeric Search Algorithm, Jilin University, Changchun, China. 2010.

(2) J.-f. Xin, X.-r. Han, F.-f. He, Y.-h. Ding, *Front. Chem.* 2019, **7**, 193.

(3) J. Lv, Y. Wang, L. Zhu, Y. Ma, *J. Chem. Phys.* 2012, **137**, 084104.

(4) Y. Wang, J. Lv, L. Zhu, Y. Ma, *Comput. Phys. Commun.* 2012, **183**, 2063–2070.

(5) F. Weigend, Phys. Chem. Chem. Phys., 2006, **8**, 1057–1065.

(6) G. E. Scuseria, C. L. Janssen and H. F. Schaefer, *J. Chem. Phys.*, 1988, **89**, 7382–7387.

(7) J. M. Tao, J. P. Perdew, V. N. Staroverov, G. E. Scuseria, *Phys. Rev. Lett.*, 2003, **91**, 146401.

(8) S. Grimme, J. Antony, S. Ehrlich, H. Krieg, *J. Chem. Phys*., 2010, **132,** 154104.

(9) J. P. Foster, F. Weinhold, *J. Am. Chem. Soc.* 1980, **102**, 7211–7218.

(10) A. E. Reed, R. B. Weinstock, F. Weinhold, *J. Chem. Phys.* 1985, **83**, 735–746.

(11) E. D. Glendening, F. Weinhold, *J. Comput. Chem.* 1998, **19**, 593–609.

(12) V. V. Zakjevskii, S. King. O. Dolgounitcheva, V. G. Zakrzewski, J. V. Ortiz, *J. Am. Chem. Soc.* 2006, **128**, 13350-13351.

(13) J. V. Ortiz, *WIREs Comput. Mol. Sci.* 2013, **3**, 123-142.

(14) M. J. Frisch, G. W. Trucks, H. B. Schlegel, G. E. Scuseria, M. A. Robb, J. R. Cheeseman, G. Scalmani, V. Barone, B. Mennucci, G. A. Petersson, H. Nakatsuji, M. Caricato, X. Li, H. P. Hratchian, A. F. Izmaylov, J. Bloino, G. Zheng, J. L. Sonnenberg, M. Hada, M. Ehara, K. Toyota, R. Fukuda, H. Borkent, W. Laarhoven, J. Hasegawa, M. Ishida, T. Nakajima, Y. Honda, O. Kitao, H. Nakai, T. Vreven, J. J. Montgomery, J. E. Peralta, F. Ogliaro, M. Bearpark, J. J. Heyd, E. Brothers, K. N. Kudin, V. N. Staroverov, R. Kobayashi, J. Normand, K. Raghavachari, A. Rendell, J. C. Burant, S. S. Iyengar, J. Tomasi, M. Cossi, N. Rega, N. J. Millam, M. Klene, J. E. Knox, J. B. Cross, V. Bakken, C. Adamo, J. Jaramillo, R. Gomperts, R. E. Stratmann, O. Yazyev, A. J. Austin, R. Cammi, C. Pomelli, J. W. Ochterski, R. L. Martin, K. Morokuma, V. G. Zakrzewski, G. A. Voth, P. Salvador, J. J. Dannenberg, S. Dapprich, D. Daniels, O. Farkas, J. B. Foresman, J. V. Ortiz, J. Cioslowski, D. J. Fox, Gaussian 16, Revision C.01, Gaussian, Inc., Wallingford, CT, 2016.

(15) G. Merino, T. Heine, G. Seifert, *Chem. Eur. J.* 2004, **10**, 4367–4371.

(16) T. Heine, R. Islas, G. Merino, *J. Comput. Chem.* 2007, **28**, 302–309.

(17) R. Islas, T. Heine, G. Merino, *Acc. Chem. Res*. 2012, **45**, 215–228.

(18) J. Jusélius, D. Sundholm and J. Gauss, *J. Chem. Phys.* 2004, **121**, 3952–3963.

(19) H. Fliegl, S. Taubert, O. Lehtonen and D. Sundholm, *Phys. Chem. Chem. Phys.* 2011, **13**, 20500–20518.

(20) D. Sundholm, H. Fliegl and R. J. F. Berger, *Wiley Interdiscip. Rev. Comput. Mol. Sci.* 2016, **6**, 639–678.

(21) M. Orozco-Ic, J. L. Cabellos, G. Merino, Aromagnetic. 2016, Cinvestav-Mérida, México.

(22) J. P. Perdew, J. A. Chevary, S. H. Vosko, K. A. Jackson, M. R. Pederson, D. J. Singh, C. Fiolhais, *Phys. Rev. B* 1992, **46**, 6671–6687.

(23) J. P. Perdew, K. Burke, M. Ernzerhof, *Phys. Rev. Lett.*, 1996, **77**, 3865-68.

(24) N. Godbout, D.R. Salahub, J. Andzelm, E. Wimmer, Can. *J. Phys.* 1992, **70**, 560.

(25) J. M. Millam, V. Bakken, W. Chen, W. L. Hase, H. B. Schlegel, *J. Chem. Phys.* 1999, **111**, 3800–3805.